Drosophila germ-line modulation of insulin signaling and lifespan

Thomas Flatt[†], Kyung-Jin Min[†‡], Cecilia D'Alterio[§], Eugenia Villa-Cuesta[†], John Cumbers[†], Ruth Lehmann[¶], D. Leanne Jones[§], and Marc Tatar[†‖]

[†]Division of Biology and Medicine, Department of Ecology and Evolutionary Biology, Brown University, Box G-W, Providence, RI 02912; [‡]Department of Biological Sciences, University of Alaska, Anchorage, AK 99508; [§]The Salk Institute for Biological Studies, Laboratory of Genetics, 10010 N. Torrey Pines Road, La Jolla, CA 92037; and [¶]Howard Hughes Medical Institute, Developmental Genetics Program, Skirball Institute of Biomolecular Medicine and Department of Cell Biology, New York University School of Medicine, New York, NY 10016

Edited by Allan C. Spradling, Carnegie Institution of Washington, Baltimore, MD, and approved March 6, 2008 (received for review September 25, 2007)

Ablation of germ-line precursor cells in *Caenorhabditis elegans* extends lifespan by activating DAF-16, a forkhead transcription factor (FOXO) repressed by insulin/insulin-like growth factor (IGF) signaling (IIS). Signals from the gonad might thus regulate whole-organism aging by modulating IIS. To date, the details of this systemic regulation of aging by the reproductive system are not understood, and it is unknown whether such effects are evolutionarily conserved. Here we report that eliminating germ cells (GCs) in *Drosophila melanogaster* increases lifespan and modulates insulin signaling. Long-lived germ-line-less flies show increased production of *Drosophila insulin-like peptides* (*dilps*) and hypoglycemia but simultaneously exhibit several characteristics of IIS impedance, as indicated by up-regulation of the *Drosophila* FOXO (dFOXO) target genes *4E-BP* and *l(2)efl* and the insulin/IGF-binding protein *IMP-L2*. These results suggest that signals from the gonad regulate lifespan and modulate insulin sensitivity in the fly and that the gonadal regulation of aging is evolutionarily conserved.

aging | endocrine regulation | reproduction | longevity | metabolism

Aside from dietary restriction, inhibition of reproduction is one of the most effective ways to extend animal lifespan (1–3). Despite the generality of this effect, the mechanisms by which reproduction regulates aging remain unknown (4–6). Progress toward this goal has been made with the nematode *Caenorhabditis elegans* (7–9). Ablation of germ-line precursor cells is sufficient to extend lifespan, and overproliferation of germ cells (GCs) shortens lifespan. In contrast, ablation of the entire gonad has no impact on longevity (7–8). These observations suggest that there is a balance between longevity assurance signals from the somatic gonad and signals from the germ line that promote aging (7). Longevity extension by germ-line ablation depends on DAF-16, the *C. elegans* ortholog of the forkhead transcription factor (FOXO), which is also required for longevity extension by reduced insulin/insulin-like growth factor (IGF) signaling (IIS) (7–8). To date, however, little is known about how signals from reproductive tissues systemically affect lifespan and whether the model developed in *C. elegans* is relevant to animals beyond the nematode (4–6, 9). Here we investigate this problem in the fruit fly, *Drosophila melanogaster*.

Several methods to inhibit reproduction extend *Drosophila* lifespan: removing oviposition substrate (10), reducing egg production (10–13), and inhibiting mating (14, 15). However, reproduction can also be reduced without affecting lifespan (3, 16–19), and whether loss of GCs extends fly lifespan remains unclear (4). Irradiation or the female-sterile mutation ovo^{D1} induce sterility and extend lifespan (12, 13), but whether these manipulations do so because they damage GCs or disrupt processes upstream of germ-line activity is unknown (4, 20, 21). Interestingly, a recent study suggests that GC ablation might not extend lifespan in *D. melanogaster* (21). Failure to form primordial GCs in *grandchildless*-like mutants (*tudor*, *germ cell-less*, *oskar*) increases lifespan only slightly or not at all (ref. 21 and our unpublished data). However, this finding is at odds with the observation that lack of a primordial germ line in a *Drosophila subobscura grandchildless* mutant extends lifespan (11, 22). Thus, in contrast to the worm, how reproductive processes modulate aging in the fly remains poorly understood (3–5, 23).

One reason for the discrepancies in fly studies might be that some *grandchildless*-like mutations impact the development of the somatic gonad (21, 24), perhaps precluding the capacity of this tissue to produce longevity assurance signals (7, 21). If so, GCs might modulate aging, but only when the somatic gonad has matured in the presence of the germ line during development. Moreover, because *grandchildless*-like mutants act during development (25), their impact on adult demography might involve pleiotropic effects independent of aging (5, 21). We therefore sought an alternative system that eliminates GCs exclusively in late development or the adult to test whether the *D. melanogaster* germ line modulates aging.

Here we investigate the impact of GC loss induced through misexpression of *bag of marbles* (*bam*). In females, *bam* is necessary and sufficient for differentiation of GCs, and overexpression of bam^+ in GCs leads to precocious differentiation and subsequent loss of GCs (26–28). In males, *bam* limits mitotic amplification divisions of spermatogonia, which occur before the initiation of terminal differentiation into spermatocytes. Overexpression of bam^+ in early male GCs causes GC loss, presumably through apoptosis (29). By manipulating *bam*, we investigate the impact of GC ablation on aging and find that loss of GCs in female and male flies extends lifespan and modulates insulin signaling.

Results and Discussion

Ectopic misexpression of bam^+ in the female germ line, by using the binary GAL4>UAS system or heat shock-induction, eliminates GCs (Fig. 1) (27, 28). Previous data suggest that the lost GCs are germ-line stem cells (GSCs): heat shock-induced bam^+ expression causes GC loss, but GCs that were not GSCs at the time of heat shock develop normally (27). Although *grandchildless*-like mutants lack pole cells and cannot form primordial GCs (21–22, 25, 30), heat shock-induced bam^+ overexpression eliminates female GSCs in the third larval instar (L3) or later but not before the L3 stage (27). When driving constitutive overexpression of UASp-bam^+ (28) with the germ-line-specific *nanos* (*nos*)-GAL4::VP16 driver (31), we found that GC loss continues in adult females, after the ovary has completed development. Females initially have the capacity to lay a small number of eggs but become fully sterile by day 7 [Fig. 1 and supporting information (SI) Fig. S1]. Similarly, in males, bam^+ overexpression induced GC depopulation in the L3 stage or later

Author contributions: T.F., R.L., D.L.J., and M.T. designed research; T.F., K.-J.M., C.D., E.V.-C., J.C., and D.L.J. performed research; R.L. and D.L.J. contributed new reagents/analytic tools; T.F. analyzed data; and T.F., R.L., D.L.J., and M.T. wrote the paper.

The authors declare no conflict of interest.

This article is a PNAS Direct Submission.

‖To whom correspondence should be addressed. E-mail: marc_tatar@brown.edu.

This article contains supporting information online at www.pnas.org/cgi/content/full/0709128105/DCSupplemental.

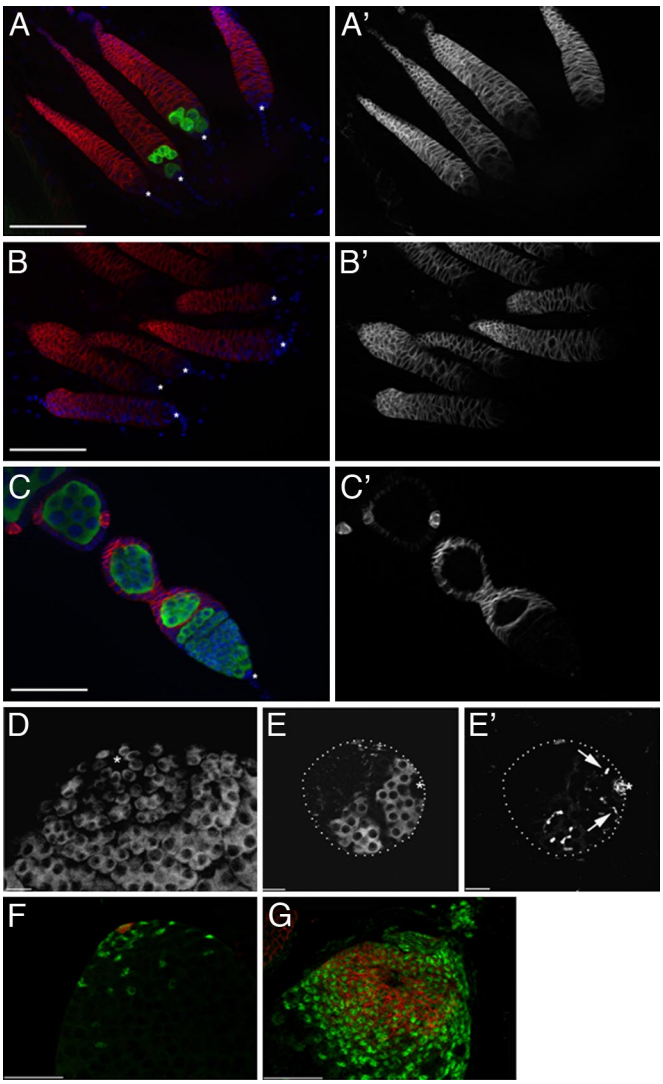

Fig. 1. GC loss and expansion of somatic cells in gonads from flies misexpressing *bam*$^{+}$. (*A–C*) GC loss in adult females misexpressing *bam*$^{+}$ in the germ line (*y w*/*w*^{1118};UASp-*bam*$^{+}$::*gfp*/+; *nos*-GAL4::VP16/+). GCs are stained for GC specific antigen vasa (green), somatic cells (FasIII, red), and DNA (DAPI, blue). Asterisk (*) denotes somatic cap cells. (*A*) GCs are rarely observed in ovarioles from 2-day-old females overexpressing *bam*$^{+}$ [24/225 ovarioles (10.7%) contained GCs]. (*B*) GC loss is virtually complete by 7 days [3/325 ovarioles (0.9%) contained GCs]. See also Fig. S1. (*C*) Germarium from a 2-day-old control female. All ovarioles from control females contained GCs at 2 ($n = 120$) and at 7 days ($n = 152$). (*A′–C′*) shows FasIII^{+} somatic cells only. Note the expanded somatic gonad in GC-less females. (*D* and *E*) GC loss in third instar larval (L3) males overexpressing *bam*$^{+}$. Control testes from L3 males (*D*) have a normal number of GSCs (vasa) in contact with hub cells (*) at the apical tip. (*E*) Males overexpressing *bam*$^{+}$ show loss of GSCs by this stage. (*E′*) GCs present near the hub have branched fusomes (arrows) as detected by staining with antibodies to α-spectrin. Note the reduced size of the gonad. Asterisk (*) denotes the FasIII^{+} apical hub. (*F* and *G*) Expansion of somatic cells in testes from adults misexpressing *bam*$^{+}$. (*F*) Control testes show normal distribution of FasIII^{+} hub cells (red) and TJ^{+} somatic cells (green). (*G*) An expansion of FasIII^{+} and TJ^{+} somatic cells is observed in testes. (Scale bars: 50 μm in *A–C*, *F*, and *G*; 20 μm in *D* and *E*.)

(Fig. 1) (29). Moreover, *bam*$^{+}$ overexpression caused a dramatic expansion of somatic cells in ovaries and testes (Fig. 1), reminiscent of the enlarged somatic gonads of agametic *grandchildless*-like mutants (21, 24). Thus, *grandchildless*-like mutants and flies misexpressing *bam*$^{+}$ have expanded somatic gonads but complete GC loss at different times.

GC loss induced by misexpression of *bam*$^{+}$ significantly increased lifespan in females and males, in several independent experiments

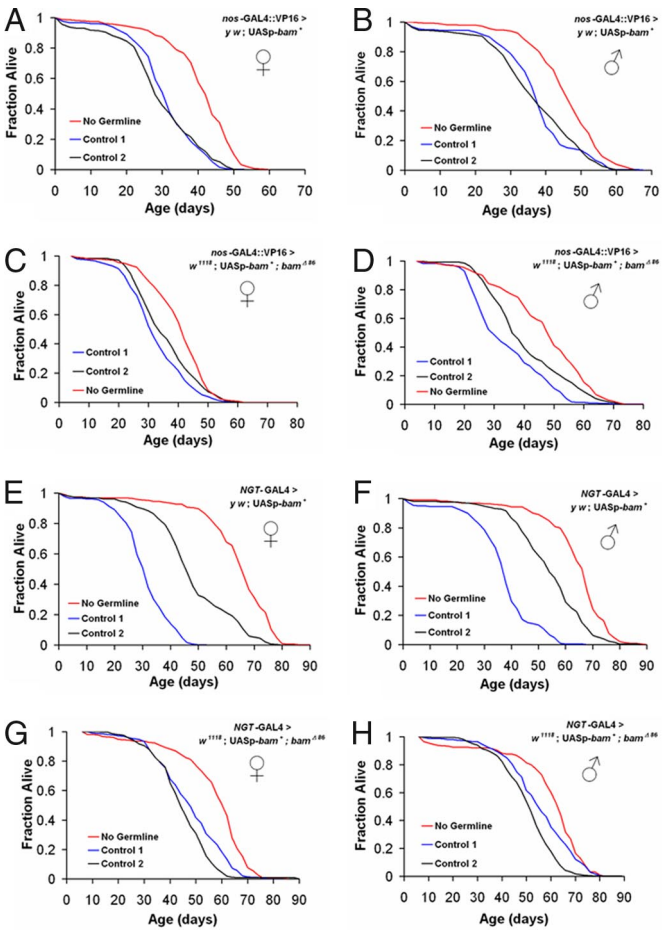

Fig. 2. Adult GC loss extends lifespan in *D. melanogaster*. (*A–D*) Driving UASp-*bam*$^{+}$ in germ line (no germ line, UASp-*bam*$^{+}$/+; *nos*-GAL4::VP16/+) extends lifespan, both in a *y w* background (*A*, females; *B*, males) and a *w*^{1118} background lacking one copy of *bam* (*C*, females; *D*, males), relative to two controls. Controls were, in the *y w* background, *y w*/*y w*;UASp-*bam*$^{+}$::*gfp*/+ (control 1) and *y w*/*w*^{1118}; *nos*-GAL4::VP16/+ (control 2), and in the *w*^{1118} background, *w*^{1118}/*w*^{1118};UASp-*bam*$^{+}$::*gfp*/+; *bam*$^{\Delta 86}$/+ (control 1) and *w*^{1118}/*w*^{1118}; *nos*-GAL4::VP16/+ (control 2). (*E–H*) Misexpressing UASp-*bam*$^{+}$ with an alternative germ-line-specific driver, *nos*-GAL4-*tubulin* (UASp-*bam*$^{+}$::*gfp*/*NGT*-GAL4), also extends lifespan, both in the *y w* background (*E*, females; *F*, males) and in a background lacking one copy of *bam* (*G*, females; *H*, males) compared with two controls (control 1: *y w*/*y w*;UASp-*bam*$^{+}$::*gfp*/+ or *w*^{1118}/*y w*;UASp-*bam*$^{+}$::*gfp*/+; *bam*$^{\Delta 86}$/+, respectively; control 2: *y w*/*y*^{1} *w**; *NGT*-GAL4/+). See Table S1 for statistics.

(Fig. 2 and Table S1). Lifespan was increased by 31.3% and 50% in females and 21% and 27.8% in males by GC ablation in a *y w* background by driving *y w*;UASp-*bam*$^{+}$ with *nos*-GAL4::VP16; effects are relative to a coisogenic control (*y w*;UASp-*bam*$^{+}$; control 1) and a control with a heterozygous background (*y w*/*w*^{1118}; *nos*-GAL4::VP16; control 2) (Fig. 2 *A* and *B* and Table S1). Longevity was also extended when UASp-*bam*$^{+}$ was driven by *nos*-GAL4::VP16 in an independent background (*w*^{1118}) lacking one copy of genomic *bam* (Fig. 2 *C* and *D*; Table S1). The capacity for GC ablation to extend lifespan was likewise effective with the germ-line driver *nos*-GAL4-*tubulin* (*NGT*-GAL4) (32) in the *y w* and *w*^{1118} backgrounds (Fig. 2 *E–H* and Table S1). Thus, *bam*$^{+}$ misexpression in the germ line is sufficient to force GC loss and to increase lifespan in multiple genetic backgrounds and with different germ-line drivers. Because the failure of *grandchildless*-like mutants to develop GCs has no consistent major effects on lifespan (ref. 21 and our unpublished data), we hypothesize that GC loss during late

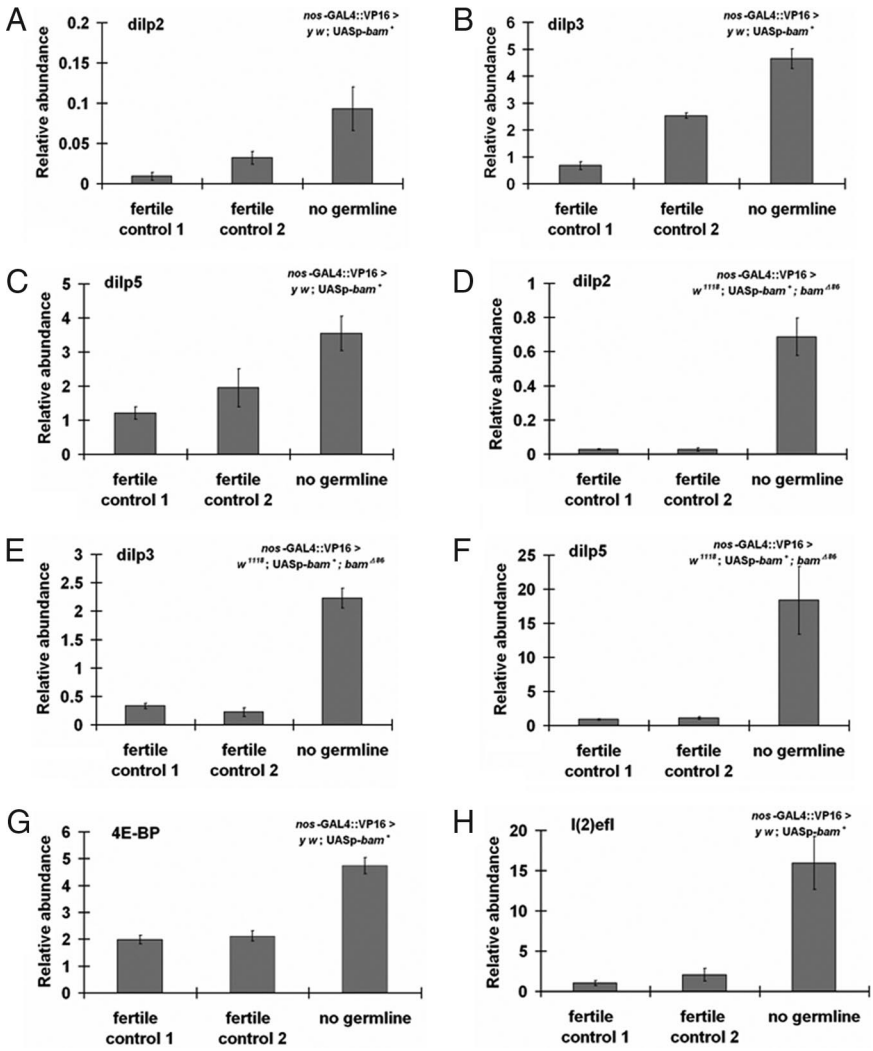

Fig. 3. GC loss up-regulates *dilp* message but activates expression of dFOXO target genes. (*A–D*) GC-less flies (UASp-bam^{+}/+; *nos*-GAL4::VP16/+) exhibit increased production of *dilp 2*, *dilp 3*, and *dilp 5*, both in the *y w* (*A–C*) and w^{1118} backgrounds (*D–F*), relative to controls. (*G–H*) GC loss causes up-regulation of dFOXO targets *4E-BP* (*G*) and *l (2)efl* (*H*) in both backgrounds. For details of genotypes, see Fig. 1.

development or in the adult might promote longevity because GCs associate and interact with somatic cells before loss.

If the germ line produces a signal that shortens lifespan or represses a somatic signal that extends lifespan, GC overproliferation should decrease lifespan (7). To test this prediction, we examined a sterile heteroallelic null mutant of *bam* ($bam^{\Delta 86}$/$bam^{\Delta 59}$) in which mitotically active, nondifferentiating GSCs overproliferate (26). Mutant flies were short-lived relative to two fertile controls (Fig. S2 and Table S1). Thus, eliminating GC proliferation slows aging, whereas GC overproliferation shortens lifespan in the fly, as in the nematode (7, 8). However, we cannot fully exclude the possibility that the longevity effects of *bam* are independent of its effects on GCs.

Germ-line loss might slow aging simply by abolishing the survival costs of producing gametes (1–2, 4, 21, 23). To rule out that egg production is required for GCs to shorten lifespan, we examined a female-sterile mutant of *egalitarian* (*egl*) (33). Mutants of *egl* prevent differentiation of cystoblasts into oocytes (34). Consequently, flies produce eggs with 16 rather than 15 nurse cells, and egg chambers degenerate before they acquire yolk (34). Lifespan of sterile *egl* mutant females (egl^{PR29}/egl^{wu50}) was reduced compared with fertile controls (Fig. S3 and Table S1), suggesting that oogenesis *per se* might not be sufficient for reproduction to shorten lifespan. This result adds to a growing number of cases showing that the tradeoff between reproduction and survival can be decoupled (3, 16–19, 21, 23).

In *C. elegans*, lifespan extension by GC loss requires the FOXO transcription factor DAF-16; FOXO activity is normally repressed by IIS (7–8). Because reduced IIS slows *Drosophila* aging [by mutations disrupting IIS (13, 35), constitutive activation of *Drosophila* FOXO (dFOXO) (18), or ablation of insulin-producing cells (36, 37)], we reasoned that GC loss might extend lifespan by down-regulating IIS. Accordingly, we measured message abundance for the three *Drosophila* insulin-like peptides (*dilps*) produced by median neurosecretory cells (mNSCs), the major insulin-producing cells (IPCs) in the brain of the adult (Fig. S4*A*) (38–40). Rather than reduced message from the *dilp2*, *dilp3*, and *dilp5* loci, we found that these transcripts were induced upon GC loss by 1.8- to 26-fold relative to controls, in two independent genetic backgrounds (Fig. 3 *A–C* and *D–F*).

Previous attempts to quantify DILPs by Western blot analysis have failed because of low ligand abundance (37), and current technology does not permit detection of circulating DILPs in the hemolymph. However, several observations suggest that increased *dilp* message in GC-ablated flies might be biologically meaningful. Immunostaining of brains with DILP antibody indicated that the

IPCs of GC-less flies produced as much and, in some cases, more DILP protein than controls, and DILP$^+$ staining of IPC axonal projections was strong, suggesting functional DILP transport (Fig. S4 *B–E*). Furthermore, neural DILPs homeostatically regulate sugar levels in the hemolymph (37, 40), and GC-less flies had reduced amounts of stored and circulating carbohydrates (Fig. S5 *A* and *B*).

The hyperinsulinism of GC-less flies is a paradox because lifespan should not be extended in the face of increased DILPs. Because high DILP levels should activate IIS in peripheral tissues and repress dFOXO, we measured transcripts of two major dFOXO targets from body tissue, the translational regulator *thor* (encoding 4E-BP), and the small heat shock protein *l (2)efl*, which are normally induced when IIS is repressed and dFOXO is activated (41–43). Message levels of both dFOXO targets were up-regulated in GC knockout flies (Fig. 3 *G* and *H*). Although we cannot rule out that these targets have transcriptional inputs other than dFOXO (44), flies with GC loss, despite elevated DILPs, express markers consistent with active dFOXO and reduced IIS.

Because reduced IIS causes dephosphorylation and nuclear translocation of dFOXO, nuclear accumulation of dFOXO can be used to assess IIS pathway activity. To confirm that dFOXO is active in GC-less flies, we examined its localization with immunostaining in peripheral fat body, a major site of IIS activity, and by Western blotting analysis with cell fractionation in whole-body tissue (Figs. S6 and S7). As expected, dFOXO was predominantly nuclear in GC flies, indicating that dFOXO is active. Yet, despite differential up-regulation of dFOXO targets, GC-less and control flies did not differ in nuclear dFOXO localization (Figs. S6 and S7), which suggests that GC loss might affect dFOXO activity independent of its subcellular localization, as recently found in *C. elegans* (45).

There are many mechanisms by which IIS can be impeded between the site of insulin production and FOXO-dependent responses of peripheral tissues: at the level of insulin secretion or transport and at many steps within intracellular IIS of target tissues (46, 47). To initiate an understanding of IIS impedance in GC-less flies, we explored whether GC loss might change transcript abundance of two DILP cofactors, dALS and IMP-L2 (48–50). In mammals, circulating IGFs form a complex consisting of IGF-1, IGF-binding proteins (IGF-BPs), and the liver-secreted scaffold protein acid labile substrate (ALS); by creating a pool of circulating IGFs, this ternary complex limits ligand availability (51). The *Drosophila* homolog of ALS (dALS) is expressed in DILP-expressing IPCs and the fat body (48, 52) and is up-regulated in *dFoxo* null mutants (53). Consistent with the model that dALS functions as a DILP cofactor, dALS forms a circulating trimeric complex containing DILP2 and IMP-L2, an Ig-like homolog of IGF-BP7 (48, 54). Binding of dALS requires prior formation of a dimeric complex containing DILP2 and IMP-L2 (48). In cell culture experiments, IMP-L2 binds mammalian insulin and IGF-1/-2, and fall army worm (*Spodoptera frugiperda*) IMP-L2 inhibits IIS through the human insulin receptor (55). Because overexpression of dALS and IMP-L2 can systemically antagonize DILP function and IIS in *Drosophila in vivo* (48, 49), we measured message abundance of *dALS* and *IMP-L2* upon GC loss. Although *dALS* levels did not change, *IMP-L2* message was increased 7-fold in GC-less flies (Fig. 4 *A* and *B*). Although this observation is correlational, it might suggest a potential explanation for why IIS might be impeded in GC-less flies in the face of elevated DILP production. It will be of major interest to determine whether GC loss can modulate DILP availability and IIS by affecting IMP-L2.

Together, our results show that GCs regulate aging and modulate IIS in the fly. Although future work is required to fully characterize IIS state upon GC loss, we observed that GC-less flies exhibit characteristics of both increased and decreased IIS. Increased DILPs and hypoglycemia are suggestive of increased IIS, but GC-less flies also have markers of IIS impedance. The

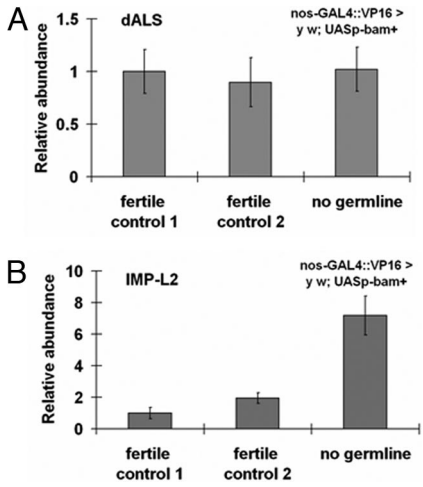

Fig. 4. GC loss up-regulates message of *IMP-L2*, but not of *dALS*. (*A*) GC loss does not alter message abundance of the DILP cofactor *dALS*. (*B*) In contrast, GC loss strongly up-regulates expression of the insulin/IGF- binding protein *IMP-L2*. See Fig. 1 for genotype information.

induction of dFOXO targets is consistent with the finding that lifespan extension by GC loss in the nematode requires FOXO/DAF-16 (7–8). In the worm, GC loss induces nuclear translocation of DAF-16 and activates DAF-16 targets, but nuclear accumulation is also observed in worms that lack the entire gonad and have normal lifespan (45). Similarly, we find that GC-less and control flies differ in dFOXO target activation, but not dFOXO localization, suggesting that IIS can affect aging by modulating FOXO/DAF-16 activity independent of subcellular localization. Indeed, dietary restriction in *C. elegans* extends longevity by activating AMP-activated protein kinase (AMPK), which phosphorylates and activates DAF-16 but does not promote DAF-16 nuclear translocation (56).

Because extended longevity by GC loss is associated with up-regulation of DILPs, GC loss might impede IIS downstream of DILP production. In humans, compensatory hyperinsulinemia is a hallmark of severe insulin resistance (57), and mutations in the tyrosine kinase domain of the insulin receptor can cause hyperinsulinemic hypoglycemia coupled with insulin resistance (58). Recent studies with fly and mouse also suggest that lifespan can be extended despite hyperinsulinemia (59, 60). In *Drosophila target-of-rapamycin* (*dTOR*) mutants, longevity extension is associated with elevated DILP2 and hypoglycemia (59), and brain-specific *insulin receptor substrate-2* (*Irs-2*) knockout mice are hyperinsulinemic but insulin-resistant and long-lived (60). Clearly, further experiments are needed to unravel the mechanisms by which insulin production can be uncoupled from IIS sensitivity and modulation of lifespan.

Our finding that GC loss affects neural DILP production also adds to growing evidence suggesting evolutionary conservation of endocrine feedback between brain and gonad (61). In *Drosophila*, neural DILPs bind to the insulin-like receptor (dINR) on GSCs to regulate GC proliferation (62, 63), and neuronal *InR* knockout (NIRKO) mice show impaired spermatogenesis and ovarian follicle maturation (64). Conversely, in rats, ovariectomy decreases IGF-1 receptor density in the brain but increases circulating IGF-1 levels (65). Together with progress made in the worm (7–9, 66) and mouse (67), the *Drosophila* system will allow us to dissect the mechanisms underlying the fundamental and intricate relationship among IIS, reproduction, and aging.

Materials and Methods

Fly Strains and Maintenance. For *bam*$^+$ misexpression, we used UASp-*bam*$^+$ in a *y w* background, obtained by backcrossing *w*; [*w*$^+$;UASp-*bam*$^+$::*gfp*]/CyO;

$bam^{\Delta 86}$/TM3 (28) for six generations into *y w* and eliminating the *bam* mutant allele. We also misexpressed bam^+ in a w^{1118} background lacking one copy of *bam* (*w*; [w^+;UASp-bam^+::*gfp*]/CyO; $bam^{\Delta 86}$/TM3). For each UAS responder, we induced expression with two germ-line-specific *nanos* (*nos*)-GAL4 lines (w^{1118}; +/+; *nos*-GAL4::VP16 [MVD1] and y^1 *w**; *NGT*-GAL4 [*nos*-GAL4-*tubulin*]) (31, 32). Thus, we examined how bam^+ misexpression affects lifespan in four sets of genotypes: (*i*) no germ line: *y w*/w^{1118};UASp-bam^+::*gfp*/+; *nos*-GAL4::VP16/+; control 1: *y w*/*y w*;UASp-bam^+::*gfp*/+; control 2: *y w*/w^{1118}; *nos*-GAL4::VP16/+; (*ii*) no germ line: w^{1118}/w^{1118};UASp-bam^+::*gfp*/+; *nos*-GAL4::VP16/$bam^{\Delta 86}$; control 1: w^{1118}/w^{1118}; UASp-bam^+::*gfp*/+; $bam^{\Delta 86}$/+; control 2: w^{1118}/w^{1118}; *nos*-GAL4::VP16/+ (control 2); (*iii*) no germ line: *y w*/y^1 *w**;UASp-bam^+::*gfp*/*NGT*-GAL4; control 1: *y w*/*y w*;UASp-bam^+::*gfp*/+; control 2: *y w*/y^1 *w**; *NGT*-GAL4 (Fig. 2 *E* and *F*); and (*iv*) no germ line: w^{1118}/y^1 *w**;UASp-bam^+::*gfp*/*NGT*-GAL4; $bam^{\Delta 86}$/+; control 1: w^{1118}/*y w*;UASp-bam^+::*gfp*/+; $bam^{\Delta 86}$/+; control 2: *y w*/y^1 *w**; *NGT*-GAL4/+. For the assay in Fig. S2, we used a heteroallelic null mutant (ry^{506} e^1 $bam^{\Delta 86}$/*red e* $bam^{\Delta 59}$) and two heterozygous controls (w^{1118}/+; *red e* $bam^{\Delta 59}$/+ and w^{1118}/+; ry^{506} e^1 $bam^{\Delta 86}$). $bam^{\Delta 59}$ is an undescribed deletion, and $bam^{\Delta 86}$ is described in ref. 26. The assay in Fig. S3 was performed with a heteroallelic mutant (*w*; *cn bw* egl^{PR29}/*cn bw* egl^{wu50}) and a control overexpressing egl^+ in the mutant (*w*; *cn bw* egl^{PR29}/*cn bw* egl^{wu50}; *CA8B*(egl^+)/+) (33, 34). UASp-bam^+, *bam* mutants, and w^{1118} were donated by D. McKearin (University of Texas Southwestern Medical Center, Dallas); *y w* by E. Rulifson (University of California, San Francisco); *nos*-GAL4::VP16 and *egl* by R.L.; *NGT*-GAL4 strain by the Bloomington Stock Center (Bloomington, IN); *dilp2*-GAL4 by E. Hafen (ETH Zürich); and UAS-*CD8*::*gfp* by R. Stocker (Université de Fribourg, Fribourg, Switzerland). Flies were reared and experiments were conducted at 25°C and 40% relative humidity on a 12-hour light–dark cycle and using a standard cornmeal/sugar/yeast/agar diet.

Gonad Immunocytochemistry. Immunofluorescence experiments on squashed testes were performed as described in ref. 29. Ovaries were dissected into PBS, fixed in fresh 4% formaldehyde/PBS for 30 min, and blocked in PAT (PBS/0.1% Triton X-100/1% BSA) for 2 h at room temperature. Primary and secondary antibodies were diluted in PAT; incubation with primary antibodies was carried out overnight at 4°C. Ovaries were washed quickly twice, followed by four 30-min washes at room temperature in PBT (PBS with 0.1% Triton X-100). Primary antibodies used were mouse monoclonal anti-fasciclin III (FasIII) (7G10) and anti-α-spectrin (3A9) at 1:10 (Developmental Studies Hybridoma Bank, University of Iowa, Iowa City, IA), rabbit anti-Vasa at 1:2,000 (gift from P. Lasko, McGill University, Montreal, QC), and guinea pig anti-Traffic jam (Tj) at 1:3,000 (gift from D. Godt, University of Toronto, Toronto, ON). Secondary antibodies were obtained from Molecular Probes. Samples were mounted in Vectashield medium with DAPI (Vector Laboratories). Images were obtained by using a Zeiss Axiovert 200 microscope and processed with Zeiss AxioVision (version 4.5) and Adobe Photoshop software.

Lifespan Assays. Adult survival was determined by using previously described methods (23, 35, 68). Newly eclosed adult flies were collected within a 24-hour period. To minimize stress-induced mortality in very young flies, we lightly anesthetized flies with moist CO_2. Each 1-liter demography cage (68) was initiated with ≈150 newly eclosed adults, mixed sexes (unless otherwise noted; Table S1). Dead flies were recorded and removed every 2 days, at which time fresh food was provided in a vial with 3 ml of medium. We used four to five replicate cages for each treatment/genotype; data were combined across replicates for each treatment/genotype. Survival, l_x, was estimated as N_x/N_0, where N_x is the number of flies alive at the beginning of each census interval and N_0 is the initial cohort size (69). We tested for significant differences in survival between pairs of cohorts using log-rank tests (69). Data were analyzed with JMP (SAS Institute) (70). We also inspected and analyzed patterns of age-specific mortality (69) to verify that differences in survival were caused by continuous differences in mortality rate (data not shown).

Quantitative PCR (qPCR). mRNA transcript levels were measured with reverse-transcription qPCR. Ten-day-old live females were snap-frozen in liquid nitrogen and stored at −80°C. Heads were separated from bodies by using a funnel with a fine mesh. For neural *dilps*, we measured message from heads, whereas for all other transcripts we measured message from decapitated bodies. Because heads can thaw rapidly and mRNA degrades, all sample preparations were performed with iced reagents and containers before RNase inactivation. We prepared total RNA from three to four replicates per genotype, each replicate with 75 heads or bodies, using TRIzol reagent (Invitrogen). The purity and amount of RNA was determined spectrophotometrically (NanoDrop, ND-1000). DNase-treated total RNA was reverse-transcribed by using the iScript cDNA synthesis kit (Bio-Rad) according to the manufacturer's protocol. For qPCR we used i*Taq* SYBR Green Supermix with ROX (Bio-Rad) and an ABI prism 7300 Sequence Detection System (Applied Biosystems). Each PCR was performed by using three to four biological replicates; each biological replicate was replicated three times (technical replicates). For each transcript, we normalized message levels relative to a GAPDH2 control by the method of $2^{-\Delta\Delta CT}$ (71). Previous work, confirmed by independent microarray analysis, suggested that GAPDH2 is a robust control when analyzing *dilp* transcript levels (18); statistical analysis of CT values of GAPDH2 controls confirmed that GAPDH2 did not differ among genotypes (Fig. S8). For information on primers see *SI Materials and Methods*.

Fecundity Assay. Details of the fecundity assay are described in *SI Materials and Methods*.

Carbohydrate Measurements. Hemolymph and total carbohydrates were measured as described (37, 40). For details see *SI Materials and Methods*.

DILP Immunocytochemistry. DILPs were detected by immunostaining of brains with DILP antibody as described (19, 72). Details are given in *SI Materials and Methods*.

FOXO Immunocytochemistry and Western Blot Analysis. We examined dFOXO subcellular localization with anti-dFOXO antibody in peripheral fat body tissue, as described in ref. 18, and in nuclear and cytosolic extracts of whole-body samples by Western blotting. Details are given in *SI Materials and Methods*.

ACKNOWLEDGMENTS. We thank H. Broihier, M. Brown, D. Godt, E. Hafen, P. Lasko, D. McKearin, E. Rulifson, R. Stocker, the Bloomington Stock Center, and the Developmental Studies Hybridoma Bank at the University of Iowa for reagents and fly stocks; J. Bauer, R. Butler, S. Morris, S. Megumi-Naylor, M. Rocha, B. Sage, D. Warburton, and R. Yamamoto for technical assistance; P. Léopold, H. Stocker, and E. Hafen for sharing results before publication; and two referees for helpful comments on the manuscript. This work was supported by National Institute on Aging (National Institutes of Health) Grants AG024360 and AG021953 (to M.T.). R.L. is a Howard Hughes Medical Institute Investigator; D.L.J. is an Ellison Medical Foundation (EMF) New Scholar; and M.T. is an EMF Senior Scholar. This research was conducted while T.F. was a Roche Research Foundation Fellow and a Swiss National Science Foundation Postdoctoral Fellow.

1. Bell G, Koufopanou V (1986) in *Oxford Surveys in Evolutionary Biology*, eds Dawkins R, Ridley M (Oxford Univ Press, Oxford), Vol 3, pp 83–131.
2. Reznick D (1985) Costs of reproduction: An evaluation of the empirical evidence. *Oikos* 44:257–267.
3. Partridge L, Gems D, Withers DJ (2005) Sex and death: What is the connection? *Cell* 120:461–472.
4. Leroi A (2001) Molecular signals versus the loi de balancement. *Trends Ecol Evol* 16:24–29.
5. Harshman LG, Zera AJ (2007) The cost of reproduction: The devil in the details. *Trends Ecol Evol* 22:80–86.
6. Tatar M (2002) Germ-line stem cells call the shots. *Trends Ecol Evol* 17:297–298.
7. Hsin H, Kenyon C (1999) Signals from the reproductive system regulate the lifespan of *C. elegans*. *Nature* 399:362–366.
8. Arantes-Oliveira N, Apfeld J, Dillin A, Kenyon C (2002) Regulation of life-span by germ-line stem cells in *Caenorhabditis elegans*. *Science* 295:502–505.
9. Mukhopadhyay A, Tissenbaum HA (2007) Reproduction and longevity: Secrets revealed by *C. elegans*. *Trends Cell Biol* 17:65–71.
10. Partridge L, Green A, Fowler K (1987) Effects of egg-production and of exposure to males on female survival in *Drosophila melanogaster*. *J Insect Physiol* 33:745–749.
11. Maynard Smith J (1958) The effects of temperature and of egg-laying on the longevity of *Drosophila subobscura*. *J Exp Biol* 35:832–842.
12. Sgro CM, Partridge L (1999) A delayed wave of death from reproduction in *Drosophila*. *Science* 286:2521–2524.
13. Clancy DJ, *et al.* (2001) Extension of life-span by loss of CHICO, a *Drosophila* insulin receptor substrate protein. *Science* 292:104–106.
14. Fowler K, Partridge L (1989) A cost of mating in female fruitflies. *Nature* 338:760–761.
15. Chapman T, Liddle LF, Kalb JM, Wolfner MF, Partridge L (1995) Cost of mating in *Drosophila melanogaster* females is mediated by male accessory gland products. *Nature* 373:241–244.
16. Marden JH, Rogina B, Montooth KL, Helfand SL (2003) Conditional tradeoffs between aging and organismal performance of Indy long-lived mutant flies. *Proc Natl Acad Sci USA* 100:3369–3373.
17. Simon AF, Shih C, Mack A, Benzer S (2003) Steroid control of longevity in *Drosophila melanogaster*. *Science* 299:1407–1410.
18. Hwangbo DS, Gersham B, Tu M-P, Palmer M, Tatar M (2004) *Drosophila* dFOXO controls lifespan and regulates insulin signalling in brain and fat body. *Nature* 429:562–566.
19. Tu M-P, Tatar M (2003) Juvenile diet restriction and the aging and reproduction of adult *Drosophila melanogaster*. *Aging Cell* 2:327–333.
20. Extavour C, Garcia-Bellido A (2001) Germ cell selection in genetic mosaics in *Drosophila melanogaster*. *Proc Natl Acad Sci USA* 98:11341–11346.
21. Barnes AI, Boone JM, Jacobson J, Partridge L, Chapman T (2006) No extension of lifespan by ablation of germ line in *Drosophila*. *Proc R Soc London Ser B* 273:939–947.

22. Spurway H (1948) Genetics and cytology of *Drosophila subobscura* IV: An extreme example of delay in gene action, causing sterility. *J Genet* 49:126–140.
23. Flatt T, Kawecki TJ (2007) Juvenile hormone as a regulator of the trade-off between reproduction and life span in *Drosophila melanogaster*. *Evolution* (*Lawrence*, *Kans*) 61:1980–1991.
24. Margolis J, Spradling A (1995) Identification and behavior of epithelial stem cells in the *Drosophila* ovary. *Development* 121:3797–3807.
25. Boswell RE, Mahowald AP (1985) Tudor, a gene required for assembly of the germ plasm in *Drosophila melanogaster*. *Cell* 43:97–104.
26. McKearin DM, Ohlstein B (1995) A role for the *Drosophila* bag-of-marbles protein in the differentiation of cystoblasts from germline stem cells. *Development* 121:2937–2947.
27. Ohlstein B, McKearin DM (1997) Ectopic expression of the *Drosophila* bam protein eliminates oogenic germline stem cells. *Development* 124:3651–3662.
28. Chen D, McKearin DM (2003) A discrete transcriptional silencer in the bam gene determines asymmetric division of the *Drosophila* germline stem cell. *Development* 130:1159–1170.
29. Schulz C, *et al.* (2004) A misexpression screen reveals effects of bag-of-marbles and TGFβ class signaling on the *Drosophila* male germ-line stem cell lineage. *Genetics* 167:707–723.
30. Williamson A, Lehmann R (1996) Germ cell development in *Drosophila*. *Annu Rev Cell Dev Biol* 12:365–391.
31. Van Doren M, Williamson AL, Lehmann R (1998) Regulation of zygotic gene expression in *Drosophila* primordial germ cells. *Curr Biol* 8:243–246.
32. Tracey WD, Jr, Ning X, Klingler M, Kramer SG, Gergen JP (2000) Quantitative analysis of gene function in the *Drosophila* embryo. *Genetics* 154:273–284.
33. Schupbach T, Wieschaus E (1991) Female sterile mutations on the 2nd chromosome of *Drosophila melanogaster*. 2 Mutations blocking oogenesis or altering egg morphology. *Genetics* 129:1119–1136.
34. Navarro C, Puthalakath H, Adams JM, Strasser A, Lehmann R (2004) Egalitarian binds dynein light chain to establish oocyte polarity and maintain oocyte fate. *Nat Cell Biol* 6:427–435.
35. Tatar M, *et al.* (2001) A mutant *Drosophila* insulin receptor homolog that extends life-span and impairs neuroendocrine function. *Science* 292:107–110.
36. Wessells RJ, Fitzgerald E, Cypser JR, Tatar M, Bodmer R (2004) Insulin regulation of heart function in aging fruit flies. *Nat Genet* 36:1275–1281.
37. Broughton SJ, *et al.* (2005) Longer lifespan, altered metabolism, and stress resistance in *Drosophila* from ablation of cells making insulin-like ligands. *Proc Natl Acad Sci USA* 102:3105–3110.
38. Brogiolo W, *et al.* (2001) An evolutionarily conserved function of the *Drosophila* insulin receptor and insulin-like peptides in growth control. *Curr Biol* 11:213–221.
39. Ikeya T, Galic M, Belawat P, Nairz K, Hafen E (2002) Nutrient-dependent expression of insulin-like peptides from neuroendocrine cells in the CNS contributes to growth regulation in *Drosophila*. *Curr Biol* 12:1293–1300.
40. Rulifson EJ, Kim SK, Nusse R (2002) Ablation of insulin-producing neurons in flies: Growth and diabetic phenotypes. *Science* 296:1118–1120.
41. Puig O, Marr MT, Ruhf ML, Tjian R (2003) Control of cell number by *Drosophila* FOXO: Downstream and feedback regulation of the insulin receptor pathway. *Genes Dev* 17:2006–2020.
42. Teleman AA, Hietakangas V, Sayadian AC, Cohen SM (2008) Nutritional control of protein biosynthetic capacity by insulin via Myc in *Drosophila*. *Cell Metab* 7:21–31.
43. Wang MC, Bohmann D, Jasper H (2005) JNK extends life span and limits growth by antagonizing cellular and organism-wide responses to insulin signaling. *Cell* 121:115–125.
44. Zhang Y, *et al.* (2008) *Caenorhabditis elegans* EAK-3 inhibits dauer arrest via nonautonomous regulation of nuclear DAF-16/FOXO activity. *Dev Biol* 315:290–302.
45. Yamawaki TM, Arantes-Oliveira N, Berman JR, Zhang P, Kenyon C (2008) Distinct activities of the germline and somatic reproductive tissues in the regulation of *Caenorhabditis elegans*' longevity. *Genetics* 178:513–526.
46. Saltiel AR, Kahn CR (2001) Insulin signalling and the regulation of glucose and lipid metabolism. *Nature* 414:799–806.
47. Biddinger SB, Kahn CR (2006) From mice to men: Insights into the insulin resistance syndromes. *Annu Rev Physiol* 68:123–158.
48. Arquier N, *et al.* (2008) *Drosophila* ALS regulates growth and metabolism through functional interaction with insulin-like peptides. *Cell Metab*, 7:333–338.
49. Honegger B, *et al.* (2008) Imp-L2, a putative homolog of vertebrate IGF-binding protein 7, counteracts insulin signaling in *Drosophila* and is essential for starvation resistance. *J Biol* 7:10.
50. Géminard C, *et al.* (2006) Control of metabolism and growth through insulin-like peptides in *Drosophila*. *Diabetes* 55 (Suppl. 2):S5–S8.
51. Boisclair YR, Rhoads RP, Ueki I, Wang J, Ooi GT (2001) The acid-labile subunit (ALS) of the 150 kDa IGF-binding protein complex: An important but forgotten component of the circulating IGF system. *J Endocrinol* 170:63–70.
52. Colombani J, *et al.* (2003) A nutrient sensor mechanism controls *Drosophila* growth. *Cell* 114:739–749.
53. Zheng X, Yang Z, Yue Z, Alvarez JD, Sehgal A (2007) FOXO and insulin signaling regulate sensitivity of the circadian clock to oxidative stress. *Proc Natl Acad Sci USA* 104:15899–15904.
54. Garbe JC, Yang E, Fristrom JW (1993) Imp-L2: An essential secreted immunoglobulin family member implicated in neural and ectodermal development in *Drosophila*. *Development* 119:1237–1250.
55. Andersen AS, Hansen PH, Schaffer L, Kristensen C (2000) A new secreted insect protein belonging to the immunoglobulin superfamily binds insulin and related peptides and inhibits their activities. *J Biol Chem* 275:16948–16953.
56. Greer EL, *et al.* (2007) An AMPK-FOXO pathway mediates longevity induced by a novel method of dietary restriction in *C. elegans*. *Curr Biol* 17:1646–1656.
57. Tritos NA, Mantzoros CS (1998) Syndromes of severe insulin resistance. *J Clin Endocrinol Metab* 83:3025–3030.
58. Hojlund K, *et al.* (2004) A novel syndrome of autosomal-dominant hyperinsulinemic hypoglycemia linked to a mutation in the human insulin receptor gene. *Diabetes* 53:1592–1598.
59. Luong N, *et al.* (2006) Activated FOXO-mediated insulin resistance is blocked by reduction of TOR activity. *Cell Metab* 4:133–142.
60. Taguchi A, Wartschow LM, White MF (2007) Brain IRS2 signaling coordinates life span and nutrient homeostasis. *Science* 317:369–372.
61. Narbonne P, Roy R (2006) Regulation of germline stem cell proliferation downstream of nutrient sensing. *Cell Div* 1:29–38.
62. LaFever L, Drummond-Barbosa D (2005) Direct control of germline stem cell division and cyst growth by neural insulin in *Drosophila*. *Science* 309:1071–1073.
63. Hsu HJ, LaFever L, Drummond-Barbosa D (2008) Diet controls normal and tumorous germline stem cells via insulin-dependent and -independent mechanisms in *Drosophila*. *Dev Biol* 313:700–712.
64. Bruning JC, *et al.* (2000) Role of brain insulin receptor in control of body weight and reproduction. *Science* 289:2122–2125.
65. El-Bakri NK, *et al.* (2004) Ovariectomy and gonadal hormone treatment: Effects on insulin-like growth factor-1 receptors in the rat brain. *Growth Horm IGF Res* 14:388–393.
66. Gerisch B, *et al.* (2007) A bile acid-like steroid modulates *Caenorhabditis elegans* lifespan through nuclear receptor signaling. *Proc Natl Acad Sci USA* 104:5014–5019.
67. Cargill SL, Carey JR, Muller H-G, Anderson G (2003) Age of ovary determines remaining life expectancy in old ovariectomized mice. *Aging Cell* 2:185–190.
68. Tatar M, Chien SA, Priest NK (2001) Negligible senescence during reproductive dormancy in *Drosophila melanogaster*. *Am Nat* 158:248–258.
69. Parmar MKB, Machin D (1995) *Survival Analysis: A Practical Approach* (Wiley, Chichester, UK).
70. Sall J, Lehman A (1996) *JMP Start Statistics: A Guide to Statistics and Data Analysis Using JMP and JMP IN Software* (SAS Institute Inc, Duxbury Press, Belmont).
71. Livak KJ, Schmittgen TD (2001) Analysis of relative gene expression data using real-time quantitative PCR and the $2^{-\Delta\Delta CT}$ method. *Methods* 25:402–408.
72. Cao C, Brown MR (2001) Localization of an insulin-like peptide in brains of two flies. *Cell Tiss Res* 304:317–321.

Supporting Information

Flatt *et al.* 10.1073/pnas.0709128105

SI Materials and Methods

Primers for Quantitative PCR (qPCR). We used the following primer pairs: *dilp2*-F, TGA GTA TGG TGT GCG AGG; *dilp2*-R, CTC TCC ACG ATT CCT TGC; *dilp3*-F, GAA CTT TGG ACC CCG TGA A; *dilp3*-R, TGA GCA TCT GAA CCG AA CT; *dilp5*-F, CAA ACG AGG CAC CTT GGG; *dilp5*-R, AGC TAT CCA AAT CCG CCA; *4E-BP*-F, GAA GGT TGT CAT CTC GGA TCC; *4E-BP*-R, ATG AAA GCC CGC TCG TAG A; *l (2)efl*-F, AGG GAC GAT GTG ACC GTG TC; *l (2)efl*-R, CGA AGC AGA CGC GTT TAT CC; *dALS*-F, TAC ATT CGG CAC CAA AAA GCT; *dALS*-R, AGA TTG GCG AAC GGC AAG T; *IMP-L2*-F, CAC TGG CTC CAA GAC CAT CT; *IMP-L2*-R, AGG TAT CGG CGG TAT CCT TT; *GAPDH2*-F, GCG GTA GAA TGG GGT GAG AC; *GAPDH2*-R, TGA AGA GCG AAA ACA GTA GC.

Fecundity Assay. For each genotype (GC-less *y w*/*y w*; UASp-*bam*$^{+}$/+; *nos*-GAL4::VP16/+; and fertile *y w*/*y w*; UASp-*bam*$^{+}$/+), we measured fecundity using 10 single adult (1-day-old) females kept with 2 *y w* males in vials containing standard fly food medium with live yeast sprinkled on top. Flies were passed daily to new vials, and fecundity was measured over 10 days posteclosion.

Carbohydrate Measurements. To measure circulating carbohydrates (glucose plus trehalose), hemolymph samples were collected from 10-day-old females by decapitating the heads. For each genotype, we collected a total of 0.3 μl of hemolymph by extracting ≈20–30 flies; hemolymph samples and standards were added to 75 μl of Infinity Glucose Reagent (ThermoElectron) in 96-well plates. To determine stored glucose (whole-body glucose), we homogenized flies in 1 ml of ice-cold homogenization buffer [0.01M KH_2PO_4, 1 mM EDTA, pH 7.4, plus protease inhibitors (CompleteMini, Roche)] and used 25 μl of homogenate to measure glucose with the Infinity Glucose Reagent. Total glucose was measured by reading absorbance at 340 nm after 3 min of incubation at 37°C. To measure trehalose in the samples, porcine kidney trehalose (Sigma Chemical, T8778) at 5 μl per 5 ml was added, the solution returned to 37°C overnight, followed by a second reading of absorbance at 340 nm. The amount of trehalose was calculated from the second absorbance reading minus that of the first reading.

DILP Immunocytochemistry. For DILP immunocytochemistry, brains of 10-day-old adult females were dissected into PBS, fixed for 1 h with fresh 4% paraformaldehyde, washed in PBS three times for 5 min, washed in PBT (PBS with 0.3% Triton X-100) three times for 20 min, and then blocked in PBT plus 1% BSA three times for 20 min at room temperature. Brains then were incubated overnight in 1:1,000 primary DILP antibody in PBT (polyclonal anti-rabbit antibody against A chain of *D. melanogaster* DILP; 440D antiserum; courtesy of M. Brown, University of Georgia) (1) at 4°C. The next day, samples were washed in PBT three times for 20 min and incubated for 2 h in 1:500 secondary antibody (Alexa Fluor 594-conjugated goat anti-rabbit IgG; Molecular Probes) in PBT at room temperature. After incubation in secondary antibody, brains were washed in PBT three times for 20 min, followed by three 5-min washes in PBS, and mounted in ProLong Gold mounting medium (Invitrogen). Images were processed using a Zeiss AxioVision Z1 fluorescent microscope with ApoTome optics (Zeiss) and Zeiss AxioVision software suite (version 4.5). The IPCs in Fig. S4*A* were visualized by overexpressing GFP under the control of a *dilp2*-GAL4 driver (*dilp2*-GAL4; UAS-*CD8*::*gfp*) (2).

FOXO Immunocytochemistry. As described in ref. 3, whole-mount samples of peripheral fat body tissue from the posterior abdomen of 10-day-old adult females were dissected into PBS, fixed in fresh 4% paraformaldehyde, incubated in anti-dFOXO (1:500, guinea pig antiserum; courtesy of H. Broihier, Case Western Reserve University), followed by incubation in Alexa Fluor 568-conjugated secondary antibody (1:2,000; Molecular Probes), and then mounted in ProLong Gold mounting medium with DAPI (Invitrogen). Samples were visualized and images processed using a Zeiss Axioplan 2 fluorescent microscope and Zeiss AxioVision software (version 4.5).

FOXO Western Blot Analysis. For each genotype, we generated lysates from 160 decapitated bodies from 10-day-old females. Cytoplasmic and nuclear extracts were prepared from lysed tissues by using the Nuclear Extract Kit (Active Motif, #40010), and protein concentration was determined with the BCA Protein Assay Kit (Pierce), following the manufacturers' protocols. For Western blot analysis, we loaded 10 μg of protein per lane using a NuPAGE 4–12% Bis-Tris Gel (Invitrogen). Antibodies used were guinea pig anti-dFOXO (a gift from H. Broihier, Case Western Reserve University), mouse anti-Lamin DMO (ADL84.12, Developmental Studies Hybridoma Bank, University of Iowa) as nuclear control, and rabbit anti-Hsp90 (SPA-846, Stressgen) as a cytoplasmic control. The intensity of each band was analyzed by using Image J software (http://rsb.info.nih.gov/ij/). For intensity analysis, the amount of dFOXO protein was corrected for nuclear contamination of the cytoplasmic fraction by quantifying and subtracting the amount of Lamin protein found in the cytoplasmic fraction.

1. Cao C, Brown MR (2001) Localization of an insulin-like peptide in brains of two flies. *Cell Tiss Res* 304:317–321.
2. Ikeya T, Galic M, Belawat P, Nairz K, Hafen E (2002) Nutrient-dependent expression of insulin-like peptides from neuroendocrine cells in the CNS contributes to growth regulation in *Drosophila Curr Biol* 12:1293–1300.
3. Hwangbo DS, Gersham B, Tu M-P, Palmer M, Tatar M (2004) *Drosophila* dFOXO controls lifespan and regulates insulin signalling in brain and fat body. *Nature* 429:562–566.
4. Broughton SJ, *et al* (2005) Longer lifespan, altered metabolism, and stress resistance in *Drosophila* from ablation of cells making insulin-like ligands. *Proc Natl Acad Sci USA* 102:3105–3110.
5. Brogiolo W, *et al* (2001) An evolutionarily conserved function of the *Drosophila* insulin receptor and insulin-like peptides in growth control. *Curr Biol* 11:213–221.
6. Rulifson EJ, Kim SK, Nusse R (2002) Ablation of insulin-producing neurons in flies: Growth and diabetic phenotypes. *Science* 296:1118–1120.

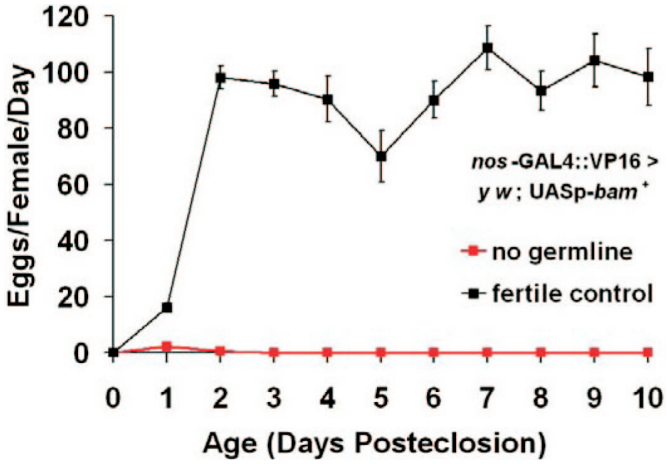

Fig. S1. GC loss causes female sterility. Early fecundity over the first 10 days posteclosion in females ectopically misexpressing *bam*$^{+}$ in the germ line (no germ line: *y w*/*y w*; UASp-*bam*$^{+}$/+; *nos*-GAL4::VP16/+) relative to a fertile control (*y w*/*y w*; UASp-*bam*$^{+}$/+). GC loss in females misexpressing *bam*$^{+}$ causes sterility but occurs after the ovary has completed its normal development. Females lay some eggs before they become fully sterile at around day 7 posteclosion. Also see Fig. 1.

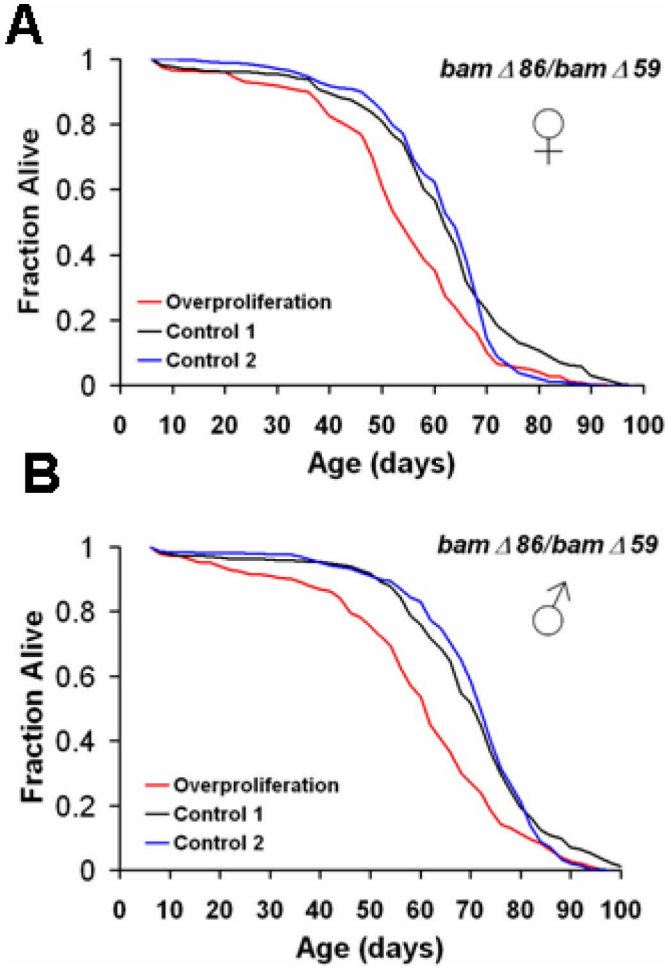

Fig. S2. GC overproliferation shortens lifespan. Survival is reduced in a heteroallelic *bam* null mutant (overproliferation: ry^{506} e^{1} $bam^{\Delta 86}$/*red e* $bam^{\Delta 59}$) compared with fertile controls (control 1: w^{1118}/+; ry^{506} e^{1} $bam^{\Delta 86}$; control 2: w^{1118}/+; *red e* $bam^{\Delta 59}$), among both females (*A*) and males (*B*). For survival statistics, see Table S1.

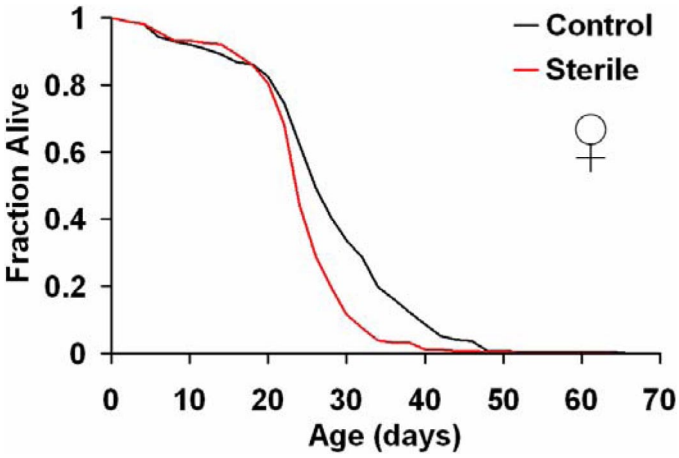

Fig. S3. Loss of oocytes is not sufficient for slowing aging. Lifespan is reduced in a female-sterile, heteroallelic mutant genotype of *egl* (sterile: *w*; *cn bw* egl^{PR29}/*cn bw* egl^{wu50}) compared with a fertile control carrying a transgenic rescue construct [control: *w*; *cn bw* egl^{PR29}/*cn bw* egl^{wu50}; *CA8B*(egl^{+})/+]. See Table S1 for survival statistics.

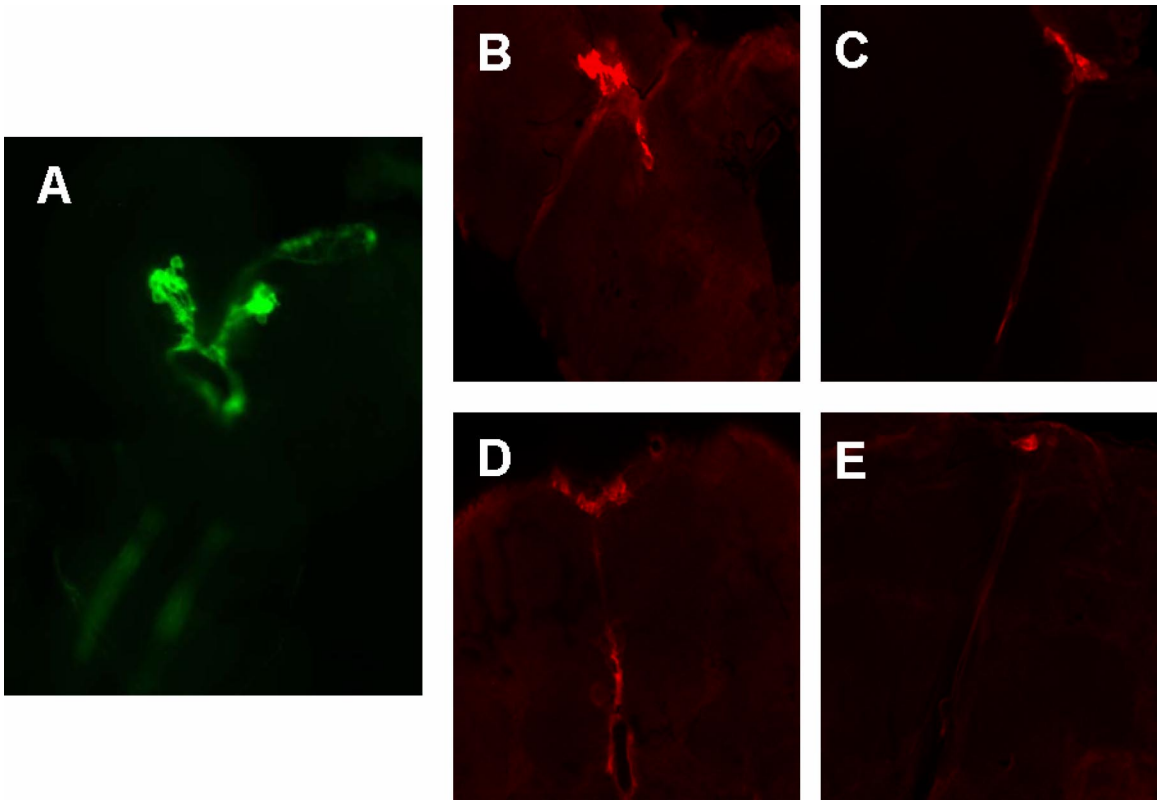

Fig. S4. DILP immunostaining of IPCs and axonal projections. (*A*) The pars intercerebralis of the fly brain contains the major insulin-producing cells (IPCs; in green, with GFP), which are functionally equivalent to the mammalian pancreatic β cells (2, 4–6). The IPCs form two bilaterally paired clusters of seven median neurosecretory cells (mNSCs), which contact the heart via axonal projections and release DILPs into the circulatory system to homeostatically regulate circulating sugar levels (4–6). The image shows the IPCs in the brain of a 10-day-old adult female fly overexpressing a GFP construct, driven with a *dilp2*-GAL4 line (*dilp2*-GAL4; UAS-*CD8*::*gfp*). (*B* and *C*) IPCs in GC-less (*y w*/*w*^{1118}; UASp-*bam*$^{+}$::*gfp*/+; *nos*-GAL4::VP16/+) flies. (*D* and *E*) IPCs in fertile control flies (*y w*/*y w*; UASp-*bam*$^{+}$::*gfp*/+). DILP protein in IPCs and their axonal projections was visualized with antiserum against DILP in 10-day-old adult females; shown are IPCs from two different individuals for each genotype. Qualitative inspection of *z* stack projections ($n = 15$ for each genotype; exposure time: 14 s) suggests that brains of GC-less flies produce as much and, in some cases, more DILP protein in the cell bodies of the IPCs than in fertile controls. Strong axonal staining is indicative of functional transport of DILP vesicles along the axon.

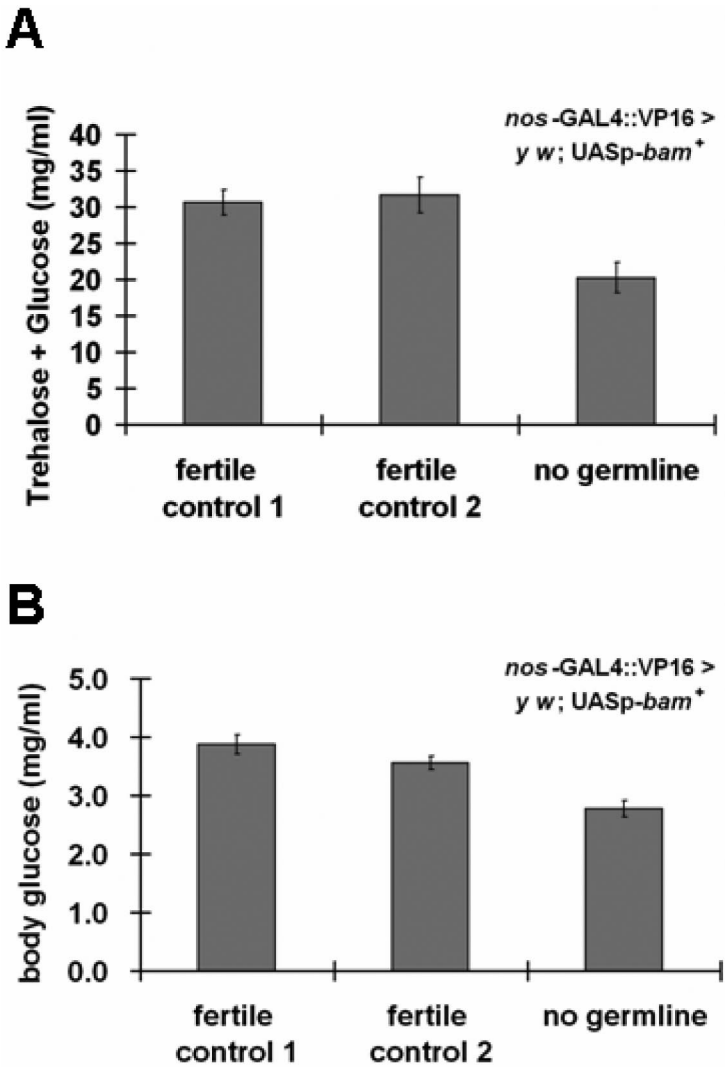

Fig. S5. GC loss lowers carbohydrate levels. In the fly hemolymph, circulating carbohydrates consist of trehalose (a glucose disaccharide) and glucose (free, monomeric glucose); together these sugars represent the combined total pool of hemolymph glucose (4, 6). (*A* and *B*) GC-less flies (*y w*/*w*^{1118}; UASp-*bam*$^{+}$::*gfp*/+; *nos*-GAL4::VP16/+) have lowered circulating levels of hemolymph glucose (glucose plus trehalose) (*A*) and exhibit a reduction in total stored glucose levels compared with fertile control flies (*y w*/*y w*; UASp-*bam*$^{+}$::*gfp*/+) (*B*). Because IPC-produced DILPs tightly regulate sugar levels in the fly (4, 6), these data suggest that increased neural DILP production in GC-less flies causes reduction in carbohydrate levels.

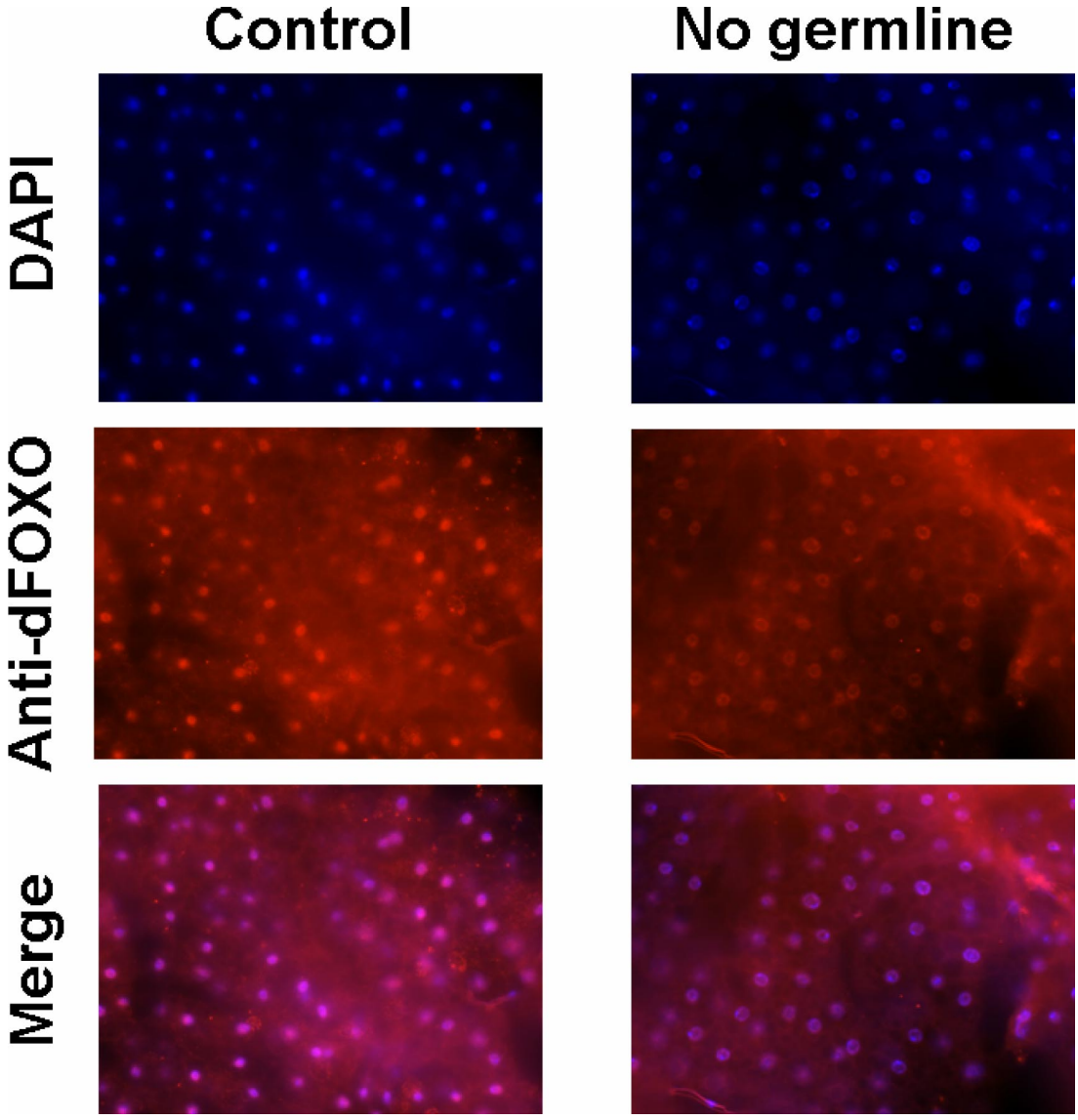

Fig. S6. Effects of GC loss on dFOXO localization in fat body. Reduced IIS can cause nuclear localization of dFOXO in target tissues, and subcellular localization of dFOXO can be used as a proxy for IIS activity (3). Peripheral fat body tissue (whole-mount tissue) of 10-day-old females was stained with anti-dFOXO antibody. In both fertile control flies (left lane; *y w*/*y w*; UASp-*bam*$^{+}$::*gfp*/+) and GC-less flies (right lane; *y w*/*w*^{1118}; UASp-*bam*$^{+}$::*gfp*/+; *nos*-GAL4::VP16/+), most fat body cell nuclei are dFOXO^{+}, suggesting that dFOXO is mainly nuclear (blue, DAPI, nuclear counterstain; red, anti-dFOXO; purple, merge), which suggests that dFOXO might be active in both GC-less and control flies (also see Fig. S7).

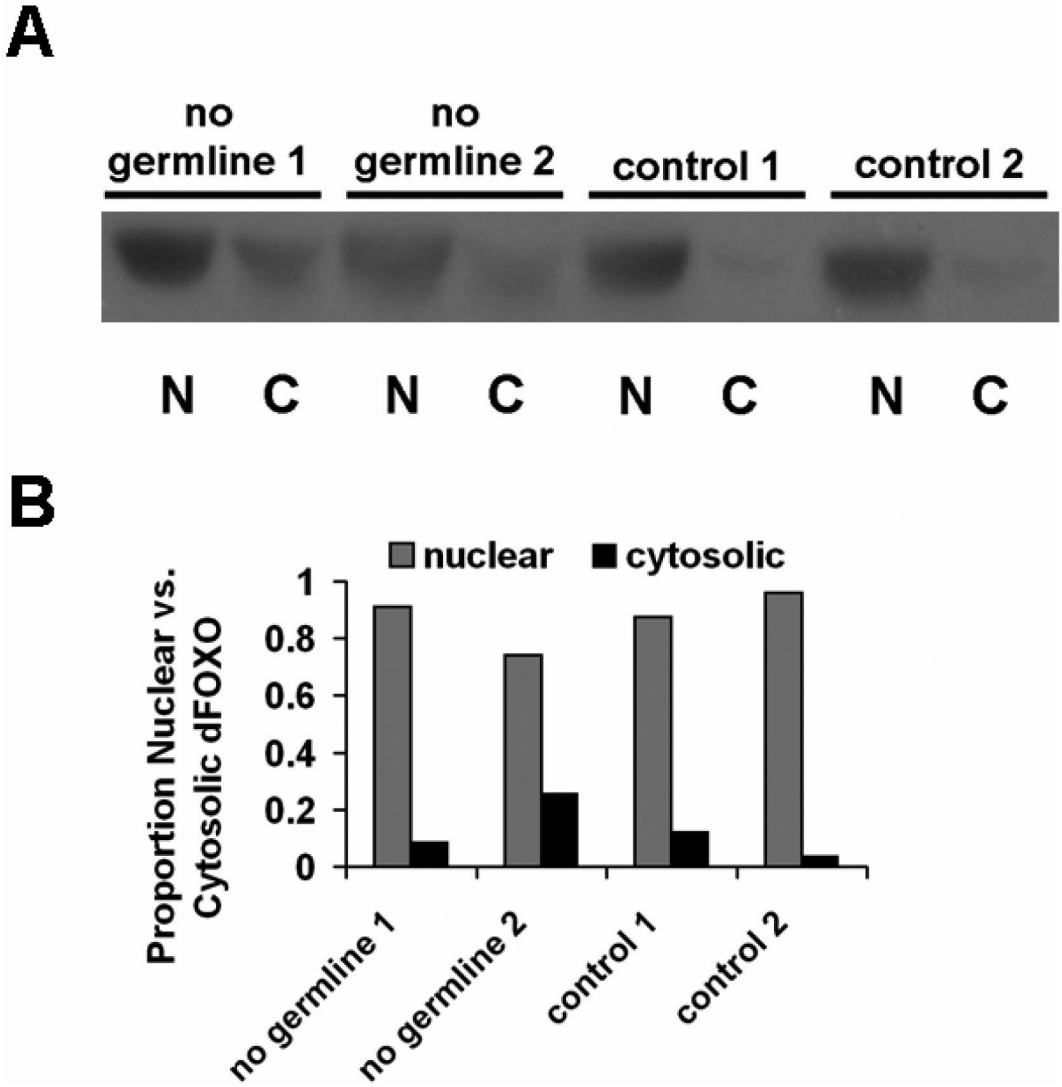

Fig. S7. Subcellular localization of dFOXO in whole-body tissue. (*A*) Western blot analysis with anti-dFOXO antibody, performed on nuclear (N) and cytosolic (C) fractions of whole bodies (without heads) of 10-day-old females. GC-less genotypes 1 and 2 have identical genotype (*y w*/*w*^{1118}; UASp-*bam*$^{+}$::*gfp*/+; *nos*-GAL4::VP16/+); however, as an internal control, crosses were set up in two ways: (*i*) by crossing UAS females to GAL4 males and (*ii*) reciprocally, by crossing GAL4 females to UAS males. Control 1 flies are *y w*/*y w*; UASp-*bam*$^{+}$::*gfp*/+; control 2 flies are *y w*/*w*^{1118}; *nos*-GAL4::VP16/+. In both GC-less and control flies, dFOXO is predominantly nuclear. (*B*) Quantification of band intensity of the Western blot shown in *A*. dFOXO is mainly nuclear, both in GC-less and control flies, suggesting that the nuclear localization pattern of dFOXO does not differ between flies with and without GC loss. Despite the lack of a difference in the nuclear localization pattern among genotypes, GC-less flies show strong up-regulation of transcriptional targets of dFOXO (Fig. 3).

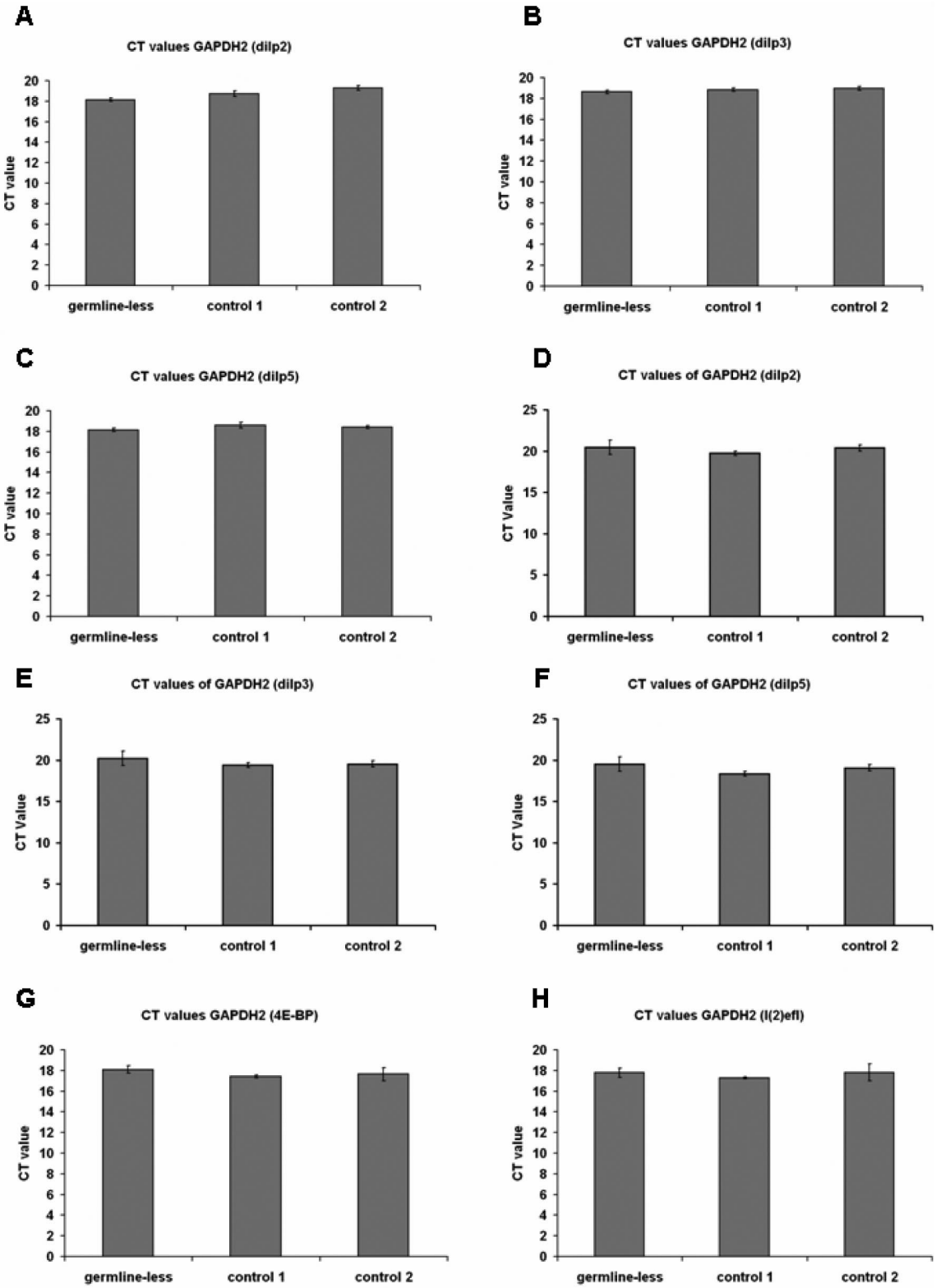

Fig. S8. CT values of GAPDH2 controls used in qPCR experiments shown in Fig. 3. (*A–H*) CT values for the GAPDH2 normalization control do not differ among GC-less flies and control genotypes 1 and 2 (one-way ANOVA with factor ''genotype'': $F_{(2,9)} > 0.29$, $P > 0.05$, in all experiments), which suggests that differences in mRNA transcript levels between flies with and without GC loss are not confounded by changes in the normalization control.

Table S1. Statistical analysis of lifespan

Genotype	Sex	Fig.	Treatment	*N*(0)	Mean lifespan	SE	Median lifespan	χ^2	*P*	Percentage change
y w/w^{1118};UASp-bam^{+}::gfp/+; nos-GAL4::VP16/+	F	2*A*	No germ line	285	40.8	0.60	42	—	—	—
y w/y w;UASp-*bam^{+}::gfp/+*	F	2*A*	Control 1	303	30.9	0.53	32	189.3	<0.0001	**31.3**
y w/w^{1118}; nos-GAL4::VP16/+	F	2*A*	Control 2	306	29.4	0.64	28	169.0	<0.0001	**50.0**
y w/w^{1118};UASp-bam^{+}::gfp/+; nos-GAL4::VP16/+	M	2*B*	No germ line	278	45.8	0.61	46	—	—	—
y w/y w;UASp-*bam^{+}::gfp/+*	M	2*B*	Control 1	237	37.1	0.78	38	67.7	<0.0001	**21.0**
y w/w^{1118}; nos-GAL4::VP16/+	M	2*B*	Control 2	290	36.4	0.77	36	67.1	<0.0001	**27.8**
w^{1118}/w^{1118};UASp-bam^{+}::gfp/+; nos-GAL4::VP16/*bam$^{\Delta 86}$*	F	2*C*	No germ line	240	40.2	0.63	42	—	—	—
w^{1118}/w^{1118};UASp-bam^{+}::gfp/+; bam$^{\Delta 86}$/+	F	2*C*	Control 1	249	32.5	0.64	32	60.2	<0.0001	**31.3**
w^{1118}/w^{1118}; nos-GAL4::VP16/+	F	2*C*	Control 2	247	35.6	0.65	34	17.7	<0.0001	**23.5**
w^{1118}/w^{1118};UASp-bam^{+}::gfp/+; nos-GAL4::VP16/*bam$^{\Delta 86}$*	M	2*D*	No germ line	312	46.8	0.82	48	—	—	—
w^{1118}/w^{1118};UASp-bam^{+}::gfp/+; bam$^{\Delta 86}$/+	M	2*D*	Control 1	300	34.0	0.72	30	130.2	<0.0001	**60.0**
w^{1118}/w^{1118}; nos-GAL4::VP16/+	M	2*D*	Control 2	323	40.4	0.72	36	29.9	<0.0001	**33.3**
y w/y^{1} w;*UASp-*bam^{+}::gfp/NGT*-GAL4,	F	2*E*	No germ line	315	63.5	0.84	66	—	—	—
y w/y w;UASp-*bam^{+}::gfp/+*	F	2*E*	Control 1	303	30.9	0.53	32	609.7	<0.0001	**100.1**
y w/y^{1} w; NGT*-GAL4	F	2*E*	Control 2	291	47.5	0.87	46	186.0	<0.0001	**43.5**
y w/y^{1} w;*UASp-*bam^{+}::gfp/NGT*-GAL4,	M	2*F*	No germ line	230	64.1	0.87	68	—	—	—
y w/y w;UASp-*bam^{+}::gfp/+*	M	2*F*	Control 1	237	37.1	0.78	38	403.5	<0.0001	**78.8**
y w/y^{1} w; NGT*-GAL4	M	2*F*	Control 2	252	53.9	0.88	56	79.3	<0.0001	**21.4**
w^{1118}/y^{1} w;*UASp-*bam^{+}::gfp/NGT*-GAL4; *bam$^{\Delta 86}$/+*	F	2*G*	No germ line	315	57.1	0.81	62	—	—	—
w^{1118}/y w;UASp-bam^{+}::gfp/+; bam$^{\Delta 86}$/+	F	2*G*	Control 1	360	47.9	0.68	48	99.4	<0.0001	**29.2**
y w/y^{1} w; NGT*-GAL4/+	F	2*G*	Control 2	354	45.0	0.58	44	225.8	<0.0001	**41.0**
w^{1118}/y^{1} w;*UASp-*bam^{+}::gfp/NGT*-GAL4; *bam$^{\Delta 86}$/+*	M	2*H*	No germ line	308	60.0	0.87	64	—	—	—
w^{1118}/y w;UASp-bam^{+}::gfp/+; bam$^{\Delta 86}$/+	M	2*H*	Control 1	337	55.5	0.75	56	18.9	<0.0001	**14.3**
y w/y^{1} w; NGT*-GAL4/+	M	2*H*	Control 2	348	50.7	0.61	52	157.8	<0.0001	**23.1**
ry^{506} e^{1} bam$^{\Delta 86}$/red e bam$^{\Delta 59}$	F	S2*A*	Overproliferation	434	51.1	0.92	54	—	—	—
w^{1118}/+; ry^{506} e^{1} bam$^{\Delta 86}$	F	S2*A*	Control 1	447	61.1	0.60	64	40.1	<0.0001	*−15.6*
w^{1118}/+; red e bam$^{\Delta 59}$/+	F	S2*A*	Control 2	406	61.2	0.83	62	60.49	<0.0001	*−13.0*
ry^{506} e^{1} bam$^{\Delta 86}$/red e bam$^{\Delta 59}$	M	S2*B*	Overproliferation	359	59.2	1.0	62	—	—	—
w^{1118}/+; ry^{506} e^{1} bam$^{\Delta 86}$	M	S2*B*	Control 1	432	68.9	0.83	72	40.8	<0.0001	*−13.9*
w^{1118}/+; red e bam$^{\Delta 59}$/+	M	S2*B*	Control 2	368	68.4	0.96	72	46.2	<0.0001	*−13.9*
w; cn bw egl^{PR29}/cn bw egl^{wu50}	F	S3	Sterile	445	31.1	0.52	32	—	—	—
w; cn bw egl^{PR29}/cn bw egl^{wu50}; CA8B(*egl^{+}*)/+	F	S3	Control	446	35.7	0.62	34	56.9	<0.0001	*−5.9*

Results grouped by experiment and sex (F, female; M, male). Reported are initial cohort size [*N*(0)]; mean lifespan, standard error (SE), and median lifespan in days; χ^2 test statistic and *P* value from log-rank test; and percentage change in median lifespan of experimental treatment relative to each control. We performed pairwise comparisons between treatment (e.g., ″no germ line″) and each control with log-rank tests. Significant increases in median lifespan relative to control are indicated in bold, and significant decreases relative to control are in italics.